Water Science & Technology

Water Science & Technology Vol 85 No 7, 2189 doi: 10.2166/wst.2022.098

Immobilization of IMP-1 metallo-beta-lactamase on Fe_3O_4@SiO_2 as nanobiocatalyst for degradation of beta-lactam antibiotics in wastewater

Mohammad javad Shokoohizadeh[a], Ali Almasi[b], Farahnaz Karami[c], Seyyed Alireza Mousavi[a] and Reza Khodarahmi[c,d,*]

[a] Department of Environmental Health Engineering, School of Public Health, Research Center for Environmental Determinants of Health (RCEDH), Health Institute, Kermanshah University of Medical Sciences, Kermanshah, Iran
[b] Social Development & Health Promotion Research Center, Health Institute, Kermanshah University of Medical Sciences, Kermanshah, Iran
[c] Medical Biology Research Center, Health Technology Institute, Kermanshah University of Medical Sciences, Kermanshah, Iran
[d] Department of Pharmacognosy and Biotechnology, Faculty of Pharmacy, Kermanshah University of Medical Sciences, Kermanshah, Iran
*Corresponding author. E-mail: rkhodarahmi@mbrc.ac.ir

ABSTRACT

Residues of antibiotics in water resources and wastewater have been significant environmental and public health problems. The current study developed a high-efficiency enzymatic nanobiocatalyst for the degradation of beta-lactam antibiotics. For this purpose, metallo-beta-lactamase IMP-1 was obtained by the cloned bla_{IMP} gene overexpressed in *Escherichia coli*. 2.6 mg purified enzyme was used for immobilization on 100 mg modified Fe_3O_4 @ SiO_2 magnetic nanoparticles. Immobilized IMP-1 showed similar storage stability to the free enzyme. The optimum temperatures and enzyme activity pH for free and immobilized enzymes were 70 °C and 60 °C, 7.5 and 6.5, respectively. In addition, after 15 reaction cycles, 80 percent of the enzyme activity was retained, according to a reusability analysis of the immobilized enzyme. For free and immobilized enzymes, the highest catalytic activity was observed for penicillin G and cephalexin, whereas Vmax/Km value for ceftriaxone was 3-fold (free enzyme) to 10-fold (immobilized enzyme) lower than for penicillin G. Also, the results showed that the immobilized IMP-1 on magnetic nanoparticles has an excellent ability to remove beta-lactam antibiotics from aqueous solutions. Thus, i could be an appropriate choice for removing beta-lactam antibiotics from pharmaceutical industry wastewater.

Key words: antibiotic removal, enzyme immobilization, nanobiocatalyst, wastewater

HIGHLIGHTS

- The IMP-1 metallo betalactamase was immobilized for the first time.
- Characterization of the free and immobilized IMP-1 metallo-beta lactamase was determined.
- Three beta-lactam antibiotics were hydrolyzed and effectively inactivated by immobilized IMP-1.
- IMP-1 nanocatalyst can be a practical solution for removal of beta lactam antibiotics from water and wastewater contaminated.

GRAPHICAL ABSTRACT

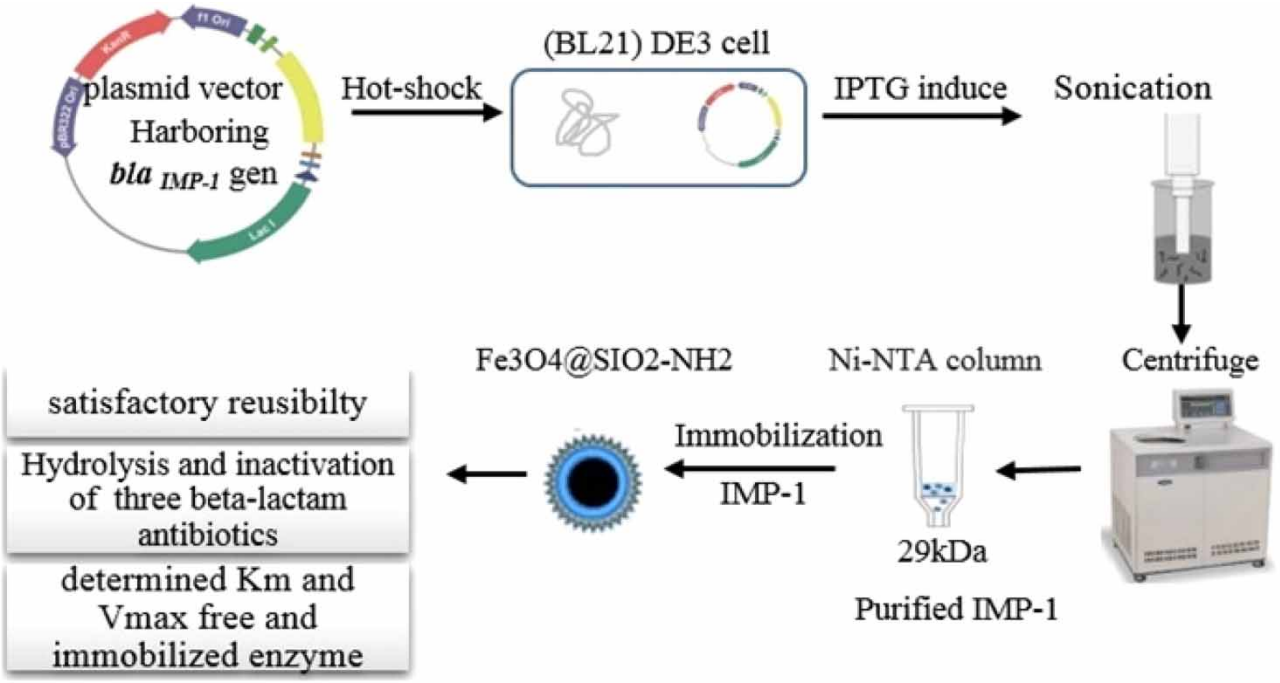

INTRODUCTION

Residues of antibiotics in water resources are important environmental and public health issues (Thai *et al.* 2018). These pollutants are discharged into the environment through various ways such as: discharged treated and untreated municipal, industrial, hospital, and livestock farming and aquaculture wastewaters. The pharmaceutical industry is one of the main sources of the release of antibiotics into water sources. Therefore, it is very important to reduce or eliminate the antibiotics released from the effluents of the pharmaceutical industry. The main concern of these substances in the environment is the development of antibiotic resistance (Rodriguez-Mozaz *et al.* 2015). With an increasing trend, tens of thousands of deaths from antibiotic resistance occur worldwide annually. Beta-lactam antibiotics are the most widely used group of prescribed antibiotics, accounting for 65% of the antibiotic market in 2003 (Elander 2003). This group includes cephalosporins, penicillin derivatives, monobactams, carbacephems, and carbapenems. The main characteristic of these antibiotics is a ring called beta-lactam in their molecular structure (De Rosa *et al.* 2021). Residues of beta-lactam antibiotics, even in very low concentrations in the environment, can lead to antibiotic resistance, and as mentioned earlier, this can cause public health and environmental problems (Lateef 2004). The Wastewater containing cephalosporin antibiotics contains inorganic salts, active pharmaceutical ingredients (APIs), and toxic organic compounds (Yang *et al.* 2016).

Biodegradation and adsorption are two major mechanisms for removing beta-lactam antibiotics, and volatilization and hydrolysis are less effective in the biological wastewater treatment processes. Conventional biological treatment methods, such as activated sludge processing, are not efficient enough to remove beta-lactam antibiotics from wastewater (Zhang *et al.* 2021). However, further treatment is required before discharging the effluent from conventional WWTPs (Pirsaheb *et al.* 2014). Recently, various advanced methods for removing beta-lactam antibiotics in wastewater and aqueous solutions have been investigated, including photolysis, ozone, ozone/hydrogen peroxide, activated carbon, nanofiltration, and reverse osmosis (Riaz *et al.* 2020). The membrane processes, such as reverse osmosis, are a relatively high-efficiency method of removing antibiotics (Couto *et al.* 2018). However, these processes have limitations, such as membrane clogging due to the formation of chemical deposits or microbial growth. In addition, this method cannot decompose antibiotics and only collect them from the liquid phase (Homem & Santos 2011). In the adsorption processes, such as membrane filtration processes, the mechanism of removing the contaminant is not decomposition and degradation, but its separation from the liquid phase and transfer to the solid (adsorbent) phase, which causes the contaminant to condense. In addition, they have limitations

such as high operating costs and regeneration of the adsorbent bed and inefficient at high concentrations of pollutants (Crini *et al.* 2019). The mentioned limitations and additional treatment of effluents and wastes from membrane filtration and adsorption processes, increased interest in studying and optimizing advanced oxidation processes. The main limitation of advanced oxidation methods, despite their high efficiency in the removal of these contaminants, is the increase in operating costs and secondary contaminants due to the production of by-products, which may sometimes be more toxic and hazardous. Studies also show that under different photolysis conditions, cephalosporin antibiotics in aqueous solutions can become more toxic and more stable products than the primary compound (Ribeiro *et al.* 2018). As a result of the mentioned problems and issues, it is necessary to develop new methods such as enzymatic processes to effectively remove beta-lactam antibiotics from wastewater (Al-Gheethi *et al.* 2015). Enzymes have been recently used as a potential biocatalyst in many biotechnological sciences (Lima *et al.* 2017). Enzymes with excellent catalytic properties have been well studied as catalysts because of their unique physicochemical behavior (Rueda *et al.* 2016). Potential advantages of enzymatic treatment compared to conventional treatment include application of biodegradable compounds, efficiency at high and low pollution concentrations, a wide range of pH, temperature and, salinity, reduction of sludge volume (without biomass production), and simplicity of process control (Pandey *et al.* 2017). The use of enzyme technology can be considered for resolving the problem of residuals of antibiotics and other emerging pollutants from water and wastewater, especially pharmaceutical industries and hospital wastewaters, due to its cost-effectiveness and specificity of removing target contaminants without producing by-products (Bilal *et al.* 2019).

Beta-lactamases are produced by some bacteria that play an important role in their resistance to beta-lactam antibiotics. These enzymes are classified into four classes and inactivate beta-lactam antibiotics due to hydrolyzing the beta-lactam ring (Gnanamani *et al.* 2017). Metallo β-lactamases are class B lactamases with three subclasses: B1, B2 and, B3. IMP-1, subclass B1, is an enzyme encoded by the transmissible bla_{IMP}-1 gene from *Pseudomonas aeruginosa.* (Mojica *et al.* 2006). For many industrial applications, enzymes must be immobilized through simple, cost-effective protocols and used for long cycles. Enzyme immobilization usually results in catalyst stability against chemical (organic solvent), temperature changes, and ionic strength.

Also, enzymes are partially denatured in aqueous solutions, which leads to a decrease in their activity. One of the challenges of enzyme immobilization is reduced enzyme activity and stability. Some immobilization methods can increase activity and resistance to inhibitors or enzyme denaturation (Melo *et al.* 2017; Monteiro *et al.* 2019). To immobilize the enzyme, various materials are used as a base or carrier (Cui *et al.* 2018). The use of silica-coated iron oxide magnetic nanoparticles has attracted much attention due to their easy separation, reuse, high dispersion and surface area, low mass transfer limitation, low toxicity, and biocompatibility for enzyme immobilization (Zhang *et al.* 2019). Direct immobilization without any cross-linking agents would cause attendant problems such as decreased enzymatic activity due to restriction of three-dimensional conformation (Chen *et al.* 2018). Glutaraldehyde is one of the most widely used materials in the design and production of biocatalysts (Barbosa *et al.* 2014). Therefore, its use as a spacer arm can have advantages such as being inexpensive and a very effective cross-linker in immobilizing the enzyme (Wahab *et al.* 2020). In most previous studies, beta-lactamase inhibitors have been investigated to reduce antibiotic resistance (Zhanel *et al.* 2013; Lomovskaya *et al.* 2020). However, only a few studies have used these enzymes to remove antibiotics from aqueous solutions (Gao *et al.* 2018). The IMP-1 was not immobilized and studied for antibiotic removal before this study. In the present work, the IMP-1 metallo-beta-lactamase was immobilized first time by covalent bonding through cross-linking in glutaraldehyde solution as a spacer arm on magnetic nanoparticles. Then the pH values and the optimum temperature of enzyme activity, thermal and stability storage, enzyme reusability, kinetic parameters, and the capacity of magnetic nanoparticles for enzyme storage were determined. This study aims to develop a novel nanobiocatalyst through immobilization of IMP-1 metallo-beta-lactamase on magnetic nanoparticles for the first time to improve the enzyme's function in the effective degradation of beta-lactam antibiotics from water solutions and contaminated wastewater, especially pharmaceutical and hospital wastewaters.

MATERIALS AND METHODS

Expression and purification of IMP-1

The recombinant IMP-1 enzyme was expressed in the *Escherichia coli* BL21 (DE3) harboring pET28a vector carrying the bla_{IMP-1} gene from *P. aeruginosa* based on the protocol Arjomandi *et al.* (2019) in the Structural Biology Laboratory of Biological Research Center of Kermanshah University of Medical Sciences. In summary, the transfer of plasmid carrying the IMP-1 gene to BL21 (DE3) cells was performed by a heat-shock method in LB (Luria Bertani) culture medium (Froger & Hall 2007).

The cells were then cultured at 37 °C in LB broth enriched with kanamycin (50 μg/ml) as selecting an agent with shaking until the optical density (OD) 600 nm reached 0.4–0.6. Protein expression was performed in the optimum condition: expression of the protein was induced by adding isopropyl-β-d-1-thiogalactopyranoside (IPTG) to a final concentration of 0.1 mM for 8 h at 25 °C. Then, for more cultivation, the culture was incubated for 2 h and centrifuged at 5,000 × g for 10 min and stored cells in −20 °C for 24 h. The cells were suspended in lysis buffer (pH 7.5) containing 50 mM Tris, 300 mM $NaCl_2$, and 5 mM imidazole. A protease inhibitor without EDTA, phenylmethylsulfonyl fluoride (PMSF) was added every 30 minutes for three times. After that, cells were disrupted by a sonicator (BANDELIN SONOPULS HD 2200, Germany). The lysate was clarified by centrifugation at 12,000 rpm for 30 min to eliminate the cell debris. Enzyme purification was performed by nickel-nitriloacetic acid (Ni-NTA) agarose affinity chromatography column according to the method of Schlesinger *et al.* (2011). Before loading the solution, the column was equilibrated by a lysis buffer as the equilibrium buffer at pH 7.5. The protein solution was then loaded onto the column. Afterward, the protein solution was dialyzed against dialysis buffer containing potassium phosphate 50 mM, NaCl 300 mM, and $ZnCl_2$ 100 μM.

Enzyme and protein assay

The purification of the enzyme was assessed by SDS-PAGE (sodium dodecyl sulfate-polyacrylamide gel electrophoresis) method (Gallagher & Wiley 2010). The enzyme solution was stored at −20 °C. During the purification procedure, beta-lactamase activity was assayed by spectroscopy by Perkin Elmer Lambda 25 UV-Visible Spectrometer at 25 °C (Waley 1974). In brief, the 500 μl of penicillin (2 mM) as a substrate was added to 497 μl of potassium phosphate buffer (50 mM) pH 7.5, then 2.8 μl (1.6 μg) of pure IMP-1 was added by appropriate shaking. After 10 min incubation, 100 μl of EDTA was added as an inhibitor of enzyme activity. IMP-1 activity was calculated by reducing the adsorption of penicillin G at a wavelength of 235 nm due to the opening of the b-lactam ring using the standard penicillin G curve that was previously prepared. Also, the enzyme concentration was determined by the Bradford method with bovine serum albumin (BSA) as standard (Bradford 1976).

Preparation of Fe_3O_4 magnetic nanoparticles

Fe_3O_4 magnetic nanoparticles were synthesized using a co-precipitation technique with some modification (Gemeay *et al.* 2020). In brief, the 4.40 g anhydrous $FeCl_3$ (0.09 mol/L) and, 3.1 g $FeSO_4{\cdot}7H_2O$ (0.045 mol/l) with a molar ratio of Fe^{2+}/Fe^{3+} (1:2) were stirred in 250 ml distilled water. The pH was increased to 11 by the addition of sodium hydroxide. The reaction was continuously overhead stirred under N_2 for 1 h at room temperature, then followed heating to 80 °C for 3 h. Afterward, the obtained magnetic nanoparticles were collected by an external magnet and washed several times with distilled water to reach a neutral pH, and finally, the nanoparticles obtained were dried in a vacuum oven for 24 hours at 60 °C.

Synthesis of magnetic silica core-shell nanoparticles (Fe_3O_4@SiO_2)

The one-step method with some modification was used to coat Fe_3O_4 with the SiO_2 shell (Lu *et al.* 2015). 0.5 g of Fe_3O_4 was dispersed in 750 ml of ethanol 96% (45 minutes ultrasonic), and then 15 ml of ammonia 25% (V/V) was added to 235 ml of distilled water and again was placed for 45 minutes in an ultrasonic bath. Afterward, 3 ml of tetraethyl orthosilicate (TEOS, 99%) was added dropwise and stirred for 8 hours at room temperature. The nanoparticles were separated by a magnet, washed several times with ethanol, and dried in a vacuum oven at 45 °C.

Amination of the Fe_3O_4@SiO_2

Magnetic silica-coated nanoparticles (Fe_3O_4@SiO_2) were functionalized (aminated) by (3-aminopropyl) triethoxysilane (APTES, 98%): 0.5 g of Fe_3O_4@SiO_2 synthesized in 50 ml of ethanol was dispersed in an ultrasonic bath for 45 minutes. 1.5 ml of APTES was added and stirred at reflux at 70 °C for 6 h. Magnetic nanoparticles (Fe_3O_4@SiO_2-NH_2) were separated by a magnet, washed several times with ethanol/acetone, and dried in a vacuum oven at 45 °C (Gemeay *et al.* 2020).

Immobilization of IMP-1 on the activated Fe_3O_4@SiO_2

Immobilization was carried out by the method of Ma *et al.* (2003) with a few modifications. Glutaraldehyde 25% was used as a coupling agent (spacer arm) to immobilize the enzyme on the magnetic nanoparticles. In summary: 100 mg Fe_3O_4 @ SiO_2-NH_2 was dispersed in 250 ml of ethanol 96% v/v, and 5% glutaraldehyde solution (V/V ratio) in 50 ml of 0.01 M sodium phosphate buffer (pH 7.4) was added to the nanoparticle/ethanol mixture. It was then incubated at 300 rpm for 12 hours at room temperature. The nanoparticles were separated by a magnet and washed several times with 50 mM potassium

phosphate (pH 7.5). Then, 10 mg of glutaraldehyde activated magnetic nanoparticles were added to a 15 ml falcon tube containing 3 ml of 50 mM sodium phosphate buffer and 2 ml of the enzyme at a 1.3 mg/ml concentration in the final concentration of 2.6 mg. It was incubated at room temperature on a puddle stirrer for 2 hours. The enzyme-carrying nanoparticles were then separated by an external magnet and washed several times with 50 mM potassium phosphate buffer (pH 7.5) containing 100 μM $ZnCl_2$. To determine the immobilization efficiency, the supernatant was collected before washing.

Determination of immobilized IMP-1 activity recovery and immobilization yield

Activity recovery and immobilization yield of immobilized IMP-1 were calculated as follows (Sheldon & van Pelt 2013):

$$\text{Activity recovery (\%)} = (\text{immobilized enzyme activity})/(\text{free enzyme activity}) \times 100 \quad (1)$$

$$\text{Immobilization yield (\%)} = (P_0 - P)/P_0 \times 100 \quad (2)$$

where,

P_0 is the protein concentration in immobilization solution; and
P is the protein concentration in the supernatant after immobilization.

Determination of the loading capacity of IMP-1 enzyme on nanoparticles

The Equation (3) was used to determine the loading capacity of the enzyme on the nanoparticles (Zhou *et al.* 2021):

$$Q = (C_1 - C_2) \times V/W \quad (3)$$

where,

Q is the loading capacity enzyme on the nanoparticles (mg enzyme/g NPs);
C_1 and C_2 are the initial concentration of the enzyme and the enzyme residual in solution after the immobilization process (mg), respectively; The enzyme concentration was measured by the Bradford method.
W is the weight of nanoparticles (mg), and V is the total volume of reaction solution (mL).

Characterization of the carrier

The FT-IR analysis was performed by a Thermo Avatar Fourier transform infrared spectrometer. The molecular and atomic crystal structure of the magnetic nanoparticles was performed at different stages of the synthesis by X-ray diffraction (PHILIPS, PW1730, X-ray diffractometer with Cu KR (λ) 0.154 nm radiation), the FESEM images, mapping, and diameter histogram were obtained by TESCAN, MIRA III operated at 10 kV electron microscope. Vibrating-sample magnetometer (VSM) analysis was carried out using an LBKFB vibrating sample magnetometer. HRTEM images were obtained by FEI, TEC9G20 high-resolution transmission electron microscopy.

Characterization of free and immobilized IMP-1

Activity assays of free and immobilized IMP-1

The activity assay of free and immobilized IMP-1 was carried out by the method of Messasma *et al.* (2018) with few modifications. Thus, a certain amount of enzyme-carrying nanoparticles were added to the final volume of 1,000 μl, including 50 mM phosphate-potassium buffer, pH 7.5, and 500 μM penicillin as a substrate, and after 5 minutes of reaction. The magnetic nanoparticles carrying the enzyme were separated by an external magnet, and the decreased absorption of the substrate was read using a spectrophotometer (Perkin Elmer Lambda 25 UV-Visible Spectrometer) at 235 nm. The reduction of a substrate concentration was determined using a standard curve. One unit of enzyme IMP-1 is the amount of enzyme that hydrolyzes one micromole of the substrate at pH 7 at 25 °C for one minute. The free enzyme activity was also measured in the same way, with the difference that at the end of the reaction time, EDTA at a concentration of 100 μmol in the reaction volume was added to complete inhibition of the enzyme activity.

Optimum temperature and pH

The activity of enzymes strongly depends on the pH and temperature of the reaction mixture. This study investigated and determined the effect of optimum temperature and pH on IMP-1 activity. Optimum temperature and pH were determined according to Schlesinger *et al.* (2011) with some modifications. 1.6 μg enzyme was incubated for 5 minutes with 1 mM penicillin G in 50 mM potassium phosphate buffer (pH 7.5 containing 100 μmol $ZnCl_2$) from 20 to 80 °C. After 5 minutes of the reaction, 100 μl of 1 mM EDTA solution was added to the reaction mixture to inhibit the enzyme activity. To determine the effect of pH on the IMP-1 enzyme activity, the free enzyme was incubated at pH 5.5–10 (citrate buffer 5.5–6, potassium phosphate buffer 6.5–8, and carbonate buffer pH 9 and 10) for 5 minutes with 1 mM of penicillin G at 25 °C. For the immobilized enzyme, as the same as the free enzyme, the optimum temperature and pH were determined, with the difference that at the end of the reaction time, the magnetic nanoparticles carrying the enzyme were separated by a magnet and the adsorption values were read by a spectrophotometer. The mean and standard deviation penicillin degradation were determined based on 3 measurements.

Thermal stability of the free and immobilized IMP-1

To determine the thermal stability, the free and immobilized enzymes were pre-incubated at 20, 30, 40, 50, 60, and 70 °C for various time intervals 15, 30, 45, and 60 minutes and at the end of these times, their activity was measured according to the previously mentioned method. Activity at 25 °C before incubation was considered as total activity and residual enzyme activity at different temperatures and times was considered as relative activity (Gao *et al.* 2018).

Reusability and storage stability

The reusability and storage stability of the immobilized IMP-1 on magnetic nanoparticles was determined according to the method of Gao *et al.* (2018). The enzyme activity was assayed after each cycle. Enzyme activity was measured in 15 consecutive cycles lasting 5 minutes at 25 °C. At the end of each hydrolysis cycle, the immobilized enzyme was separated from the reaction medium by a magnet and washed with an assay buffer. The residual activity in each cycle was expressed based on the ratio of enzyme activity to its activity in the first cycle based on the percentage (relative activity). The storage stability of the immobilized and free enzyme was determined under the same storage conditions at 4 °C for 4 weeks. At the end of each week, a certain volume of both free and immobilized enzymes was harvested and an activity assay was performed. The activity of IMP-1 at the beginning of storage was considered to be 100%.

Kinetic parameter for Pen G, CEX and CRO antibiotics

The spectrophotometric assay was used to determine the kinetic parameters of free and immobilized enzymes for penicillin G (Pen G), cephalexin (CEX), and ceftriaxone (CRO) antibiotics (Waley 1974). The different concentrations (μM) of each antibiotic at 25 °C in 50 mM potassium phosphate buffer (pH 7.5, 100 μl $ZnCl_2$) and certain concentrations of free and immobilized IMP-1 were used in the 1,000 μl final volume of the reaction. Measurement of activity was performed using of spectroscopy earlier described. Changes in the values of wavelength adsorption obtained results hydrolysis of the beta-lactam ring at 235, 260, and 241 nm were read for Pen G, CEX, and CRO, respectively. Antibiotic residual values were calculated using the slope of the standard curve line which had already been prepared. Then, using GraphPad prism (version 6), the Michaelis-Menten and Lineweaver-Burk plots were drawn and the values of V_{max} and K_m of free and immobilized enzymes were obtained. (Rodriguez *et al.* 2019).

Determining the inactivation of antibiotics

The inactivation of Pen G, CEX, and CRO after enzymatic hydrolysis was investigated by agar well diffusion according to the Clinical and Laboratory Standards Institute (CLSI) 27th ed. For this purpose, a suspension of ATCC 25922 *E. coli* with a concentration of 0.5 McFarland (108×1.58 cfu) was prepared in Müller-Hinton broth growth medium. Bacteria were seeded by the lawn culture method in the Muller-Hinton agar plates using a sterile cotton swab. Then 50 microliters of enzymatic reaction solution sterilized by filter 0.22 were added to the wells in the plates and incubated overnight at 35 °C. The inhibition zone diameter around the wells was measured, and the inhibition effect of antibiotics before and after enzymatic hydrolysis by IMP-1 was compared.

Statistical analysis

In this study, $P \leq 0.05$ was considered statistically significant. All experiments were performed independently with three replications to calculate the mean and standard deviation. All data related to immobilization are expressed as means ± standard deviation. SPSS version 16 was used for statistical analysis.

RESULTS AND DISCUSSION

In the present study, for the first time, recombinant IMP-1 metallo-beta-lactamase was immobilized on magnetic nanoparticles for the purpose of hydrolysis of beta-lactam antibiotics. The difference between the present work and a number of similar studies is shown in Table 1. Also, in the results and discussion section, the results obtained from each phase of the study were compared with the results of similar studies.

Expression and purification of IMP-1

To facilitate study and use of enzyme for the present study, the bla_{IMP} gene was cloned into a T7 expression vector (pE28a) and was overexpressed in the *E. coli* BL21 (DE3). SDS-PAGE data showed that IMP-1 was expressed successfully. The molecular weight of the IMP-1 was approximately 29 kDa as determined by SDS-PAGE (Figure 1). Crude extraction of culture was purified by a Ni-NTA column. Then, the protein was dialyzed according to the method mentioned earlier. Purification fold and % yield after this step was 2.36 ± 0.568 and 61.55 ± 6.10, respectively (Table 2). Enzymes purification is important in studying the structural and functional properties and foretelling their applications. In the present study according to the data reported in Table 3, pure enzyme yield was 31 mg per liter culture, which is more than the amount reported by

Table 1 | Comparison of present work with similar studies

Authors/year of publication	Pollutant	Method of removal	Results	Differences with the current study
Shokoohi *et al.* (2018)	Cephalexin	Enzymatic oxidation by laccase fungal and HBT as mediator	90% removal was achieved at 45 °C and one hour reaction time at pH 5.	Need for intermediate material compared to the present study and the immobilized enzyme was not used.
Zhao *et al.* (2016)	Penicillin G	Immobilized penicillinase on the ultrafiltration membrane	100% penicillin G at a concentration of 3 mg/L was removed.	A pollutant was removed in a continuous flow. In the present study, the removal of three pollutants at different concentrations was investigated as a uncontinuous flow.
Gao *et al.* (2018)	Penicillin G	Immobilized TEM-1 beta lactamase on the magnetic nanoparticles	Optimum temperature of activity of immobilized TEM-1 was 25 °C. At 50 °C, the relative activity of the immobilized enzyme was about 50%.	In the present study, the thermal and storage stability and optimum temperature of activity of free and immobilized IMP-1 were higher. Also, in comparison with the present study, the enzymatic inactivation of antibiotic has not been investigated. In addition, kinetic parameters for beta-lactam antibiotic with free and immobilized TEM-1 was not determined.
Becker *et al.* (2016)	32 antibiotics from 5 classes of antibiotics	Fungal laccase and syringe aldehyde as mediator	After 24 hours, up to 50% of the 28 antibiotics were eliminated. The mediator slowed the reaction and the toxicity increased.	Need for intermediate material compared to the present study. Also, the pollution removal reaction was time consuming (24 hours) and immobilized enzyme was not used.

Horton *et al.* (2012). The enzyme yields of purified IMP-1 were between 3 and 7 mg per liter of culture. Purification was carried out by affinity chromatography with a Strep-Tactin® Superflow® resin.

Characterization of MNPs

FT-IR spectra

FT-IR spectra analysis was used to prove the successive steps of modification and activation of the surface of magnetic nanoparticles. For all samples due to bending vibrations of Fe-O in the Fe_3O_4, the absorption band was observed at 568 cm^{-1}. Due to the surface modification of silica, a strong absorption band was observed at 1,092 cm^{-1} is straight direct evidence to verify the formation of the silica shell. Also, the absorption bands 2,918 and 2,835 cm^{-1} in the Fe_3O_4@ SiO_2 nanoparticles are related to the C-H bands as a result of the amination of them by aminopropyl (Nandiyanto *et al.* 2019). In addition, the

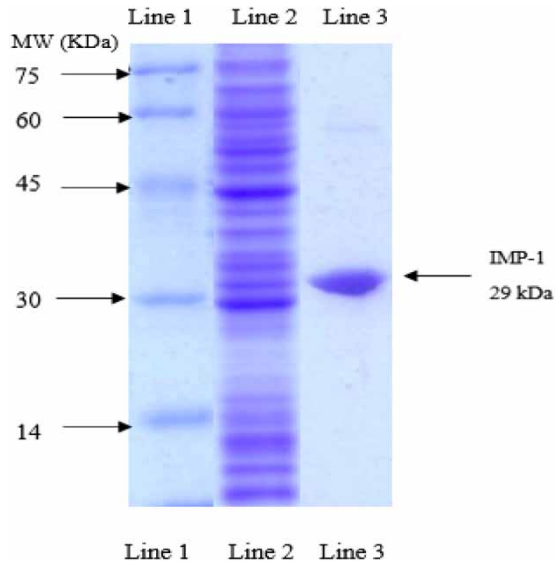

Figure 1 | SDS page gels of IMP-1: line1, protein molecular weight marker; line2, rude proteins after ultra-sonication and centrifugation in precipitation; line3, IMP-1 after Ni-NTA affinity chromatography.

Table 2 | Purification steps of the Metallo-beta-lactamase IMP-1

Purification step	Total protein(mg)	Total activity(U)	Specific activity (U/mg)	Purification fold	Yield (%)
Crud enzyme	120 ± 0.510	1,506.58 ± 146.73	12.55 ± 1.22	–	100
Ni-NA column	31 ± 0.054	921.06 ± 43.06	29.71 ± 1.390	2.36 ± 0.568	61.55 ± 6.10

Data are means ± standard deviation of three replicate.

Table 3 | Results for activity and protein assay during IMP-1 immobilization

IMP-1	Total protein(mg)	Total activity(u/ml)	Specific activity(u/mg)	Activity recovery (%)	Immobilization yield (%)	Capacity (mg protein/g nanoparticles)
Free IMP-1 in the immobilization solution	2.72 ± 0.11	29.46 ± 0.36	10.83 ± 0.19			
IMP-1 in the supernatant after immobilization	0.5 ± 0.04	1.91 ± 0.82	3.82 ± 0.17			
Immobilized IMP-1	2.21 ± 0.006	7.65 ± 0.068	3.4615 ± 0.001	25.96 ± 1.54	81.61 ± 0.14	221± 0.67

Data are means ± standard deviation of three replicate.

absorption of primary amine may overlap by the O-H band at 3,400–3,500 and 1,630, respectively (Figure 2(a)). The results show that the modification of MNPs with the amine group was performed successfully, consistent with the results of similar studies (Chen *et al.* 2008).

XRD analysis

The X-ray diffraction patterns were used to study the crystal structure of all nanoparticle samples and are shown in Figure 2(b). XRD diagram for bare Fe_3O_4 nanoparticles, peaks appeared in 2θ: 30.3° (220), 35.9° (311), 43.3° (400), 57.1° (511), and 63.10° (440) except for the peak existed at $2\theta = 18°$, which might be attributed to the existence of amorphous SiO2, no other significant peaks can be observed.Were in accordance with the database of Fe_3O_4 in the JCPDS (JCPDS card: 19–629) file. These results indicate that Fe_3O_4 crystal is a highly crystalline cubic spinel structure. Similar peaks were observed for other nanoparticle samples, indicating the stability of the crystal structure of nanoparticles during the silica coating process, amine functionalization, and glutaraldehyde activation. These results are coordinated with other studies. (Fang *et al.* 2016; Feyzi & Norouzi 2016).

VSM analysis

The results of the VSM analysis of nanoparticle samples are shown in Figure 3. According to the results, all 4 samples are super magnetic, and the highest amount of magnetic saturation is 73.5 emu/g, which belongs to Fe_3O_4. In addition, despite the decrease in the amount of magnetic saturation in other samples due to coating and functionalization, they have

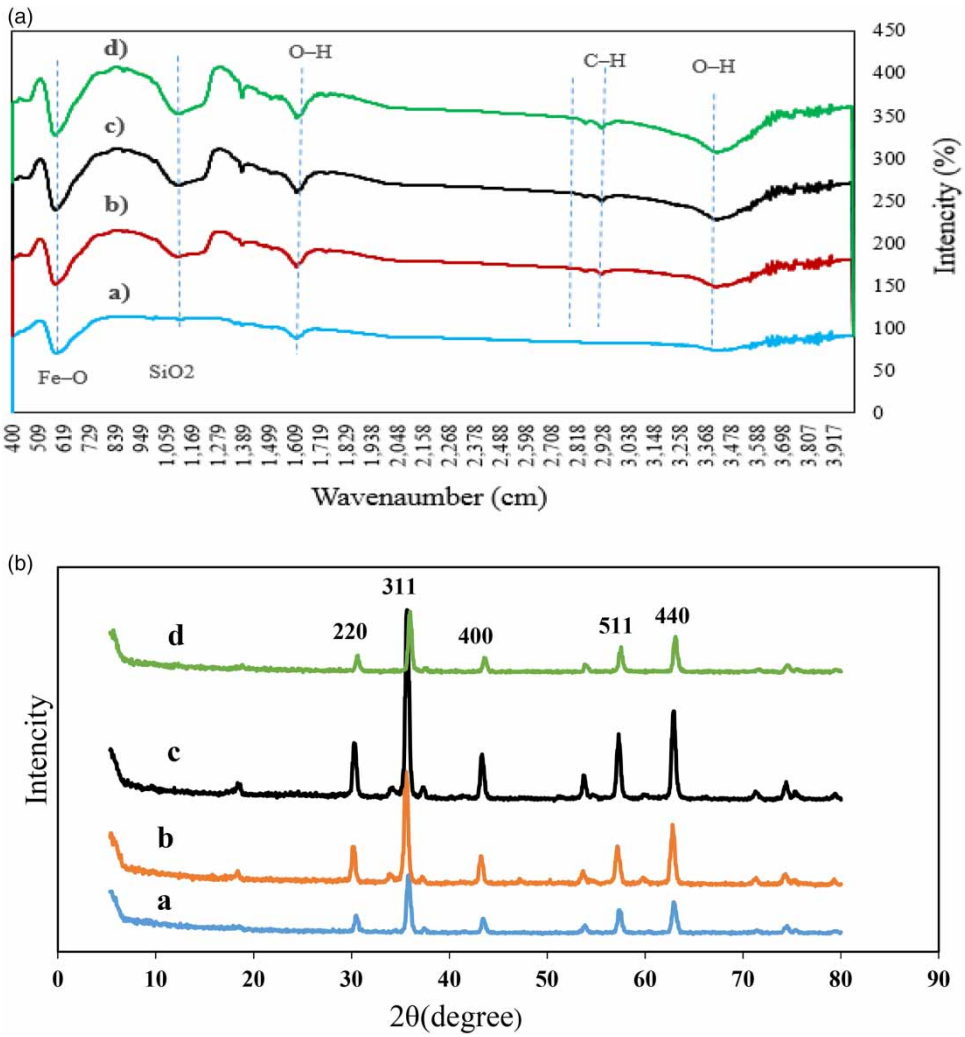

Figure 2 | (a) FT-IR spectra and (b) XRD patterns of: Fe_3O_4 (a), Fe_3O_4@SiO_2 (b), and Fe_3O_4@SiO_2–NH_2 (c) and MNPs immobilized IMP-1 (d).

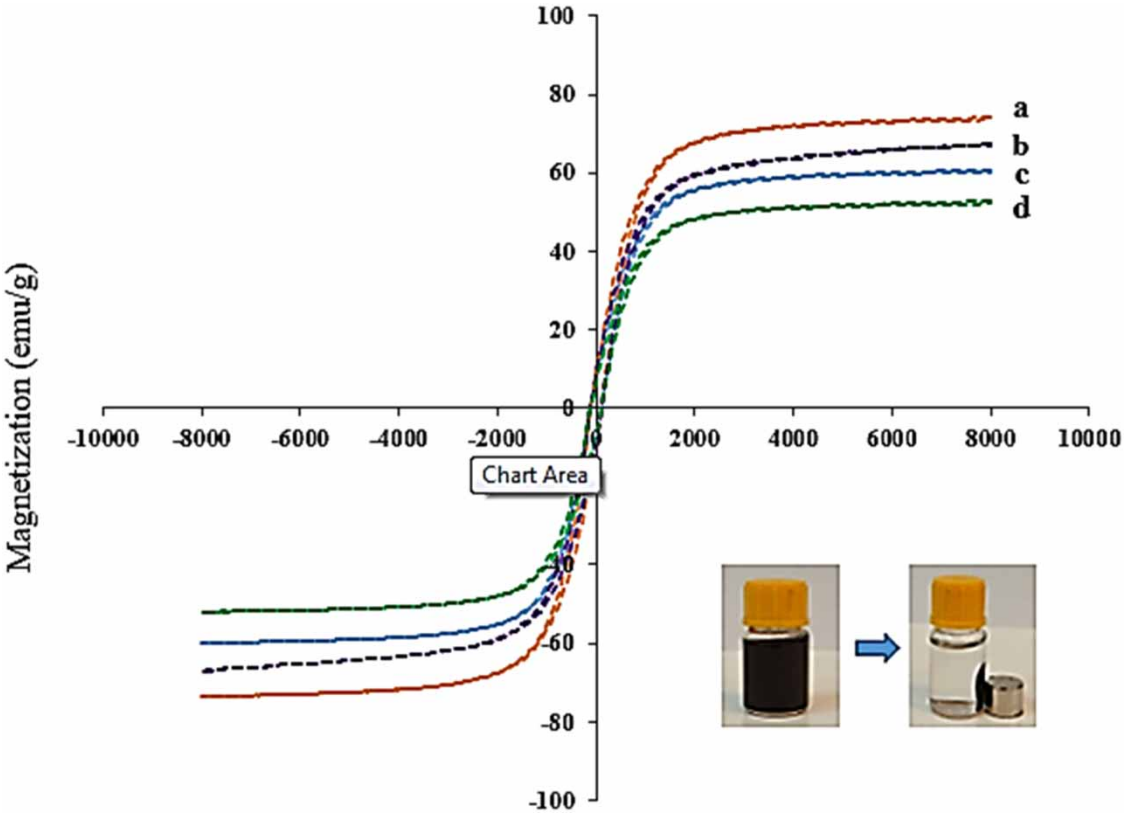

Figure 3 | VSM magnetization curves of the Fe_3O_4 (a), Fe_3O_4@SiO_2 (b), and Fe_3O_4@SiO_2– NH_2 (c) and MNPs immobilized IMP-1 (d).

appropriate magnetic properties, which are consistent with the results of other similar studies (Ghasemzadeh *et al.* 2015; Alemi-Tameh *et al.* 2016). Therefore, these nanoparticles can be used for enzyme immobilization purposes due to their ease of separation from a reaction solution. Magnetic separation provides a very convenient approach for removing and recycling magnetic biocatalysts. This feature provides reusability and convenience of operational processing.

Scanning electron microscope (SEM) and HRTEM

The morphology and size of the nanoparticles by FESEM are shown in Figure 4. The results showed that the nanoparticles were spherical in shape, and the size of Fe_3O_4@SiO_2 and Fe_3O_4@SiO_2-NH_2 as a result of coating with TEOS and amination by APTES were larger than bare Fe_3O_4 nanoparticles. HRTM images also showed that a clear thin layer of silica formed around the nanoparticles. (Figure 5). This showed that SiO_2 was successfully coated on Fe_3O_4 nanoparticles. Similar results have been reported in the study of Wang *et al.* (2012).

EDS analysis

EDS analysis was performed for all samples of magnetic nanoparticles at different stages of synthesis, coating, amination, and activation by glutaraldehyde. The elementary composition of Fe_3O_4@SiO_2-NH_2 nanoparticles including iron, oxygen, silicon, carbon, and nitrogen proved by the EDS spectrum (Figure 6). These results show no other elements in the nanoparticle composition and the main elements are evenly distributed in the nanoparticle composition. It also further proves the synthesis of Fe_3O_4@SiO_2-NH_2. The results obtained from the EDS analysis of the present study are consistent with the results of the study of Alemi Tameh *et al.* (2016).

Immobilization of IMP-1

The IMP-1 metallo-beta-lactamase was immobilized by covalent bonding through cross-linking in glutaraldehyde solution as a spacer arm on magnetic nanoparticles. Thus, a covalent bond was established between the aldehyde agent glutaraldehyde and the enzyme amino enzyme. To determine the optimum condition for the immobilization process, different times were

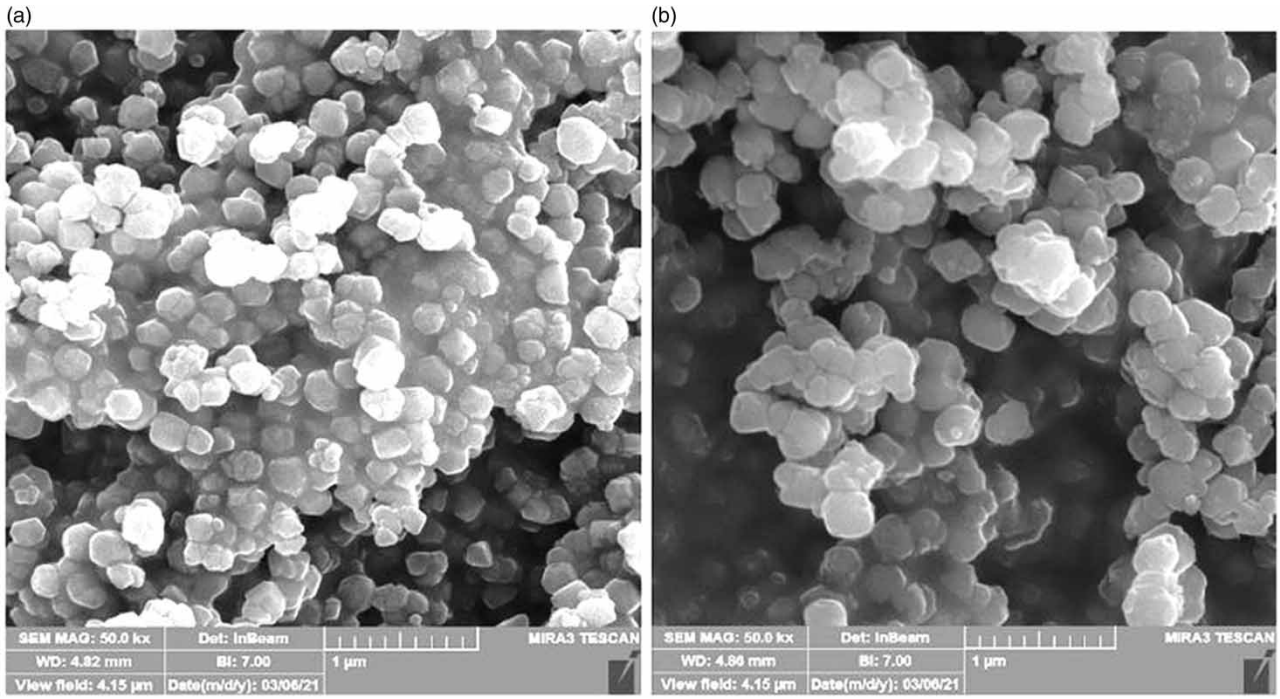

Figure 4 | FESEM images of Magnetic nanoparticles: Fe_3O_4 (a) and Fe_3O_4@SiO_2 –NH_2 (b).

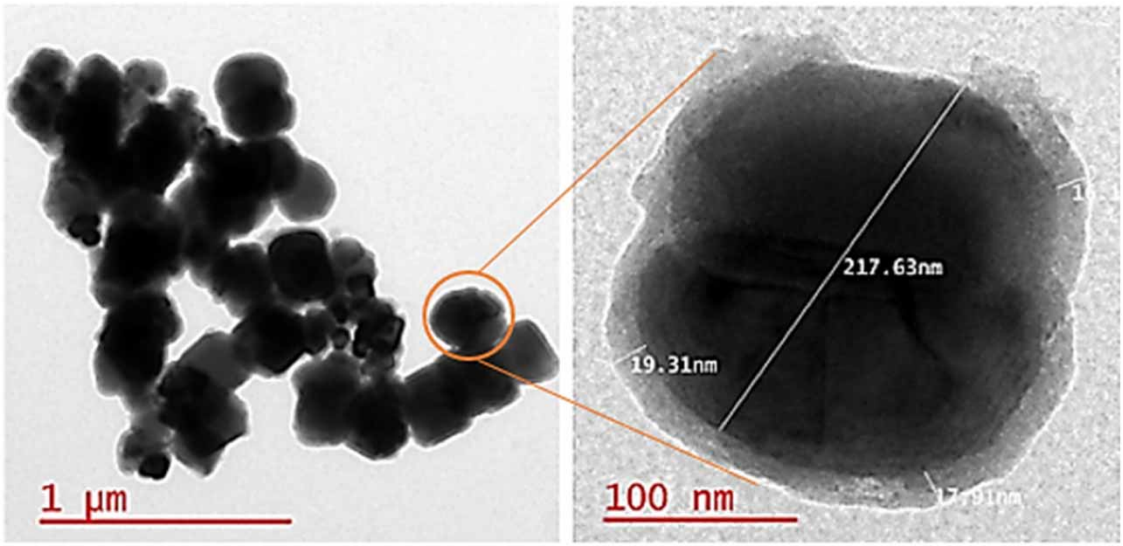

Figure 5 | HRTEM images of core-shell magnetic nanoparticles immobilized IMP-1.

examined and optimum temperature was selected from literature. In addition to determining the optimum concentration of the enzyme, three concentrations were checked. Also, to reduce diffusion limitation, the strategy of amine-functionalized magnetic nanoparticles was used.

The IMP-1 immobilization data are shown in Table 3. The enzyme was added to the nanoparticles in three 0.17, 0.338, and 0.6775 mg/ml concentrations. At concentrations of 0.17 and 0.338 mg/ml of enzyme, activity recovery was 26.94% and 26.71%, respectively. The immobilization yield was 100%, however, at the concentration of 0.6775 mg/ml, the activity recovery was 25.96% and the immobilization yield was 81.61 $\pm$ 0.14%. The results showed that the immobilization yield

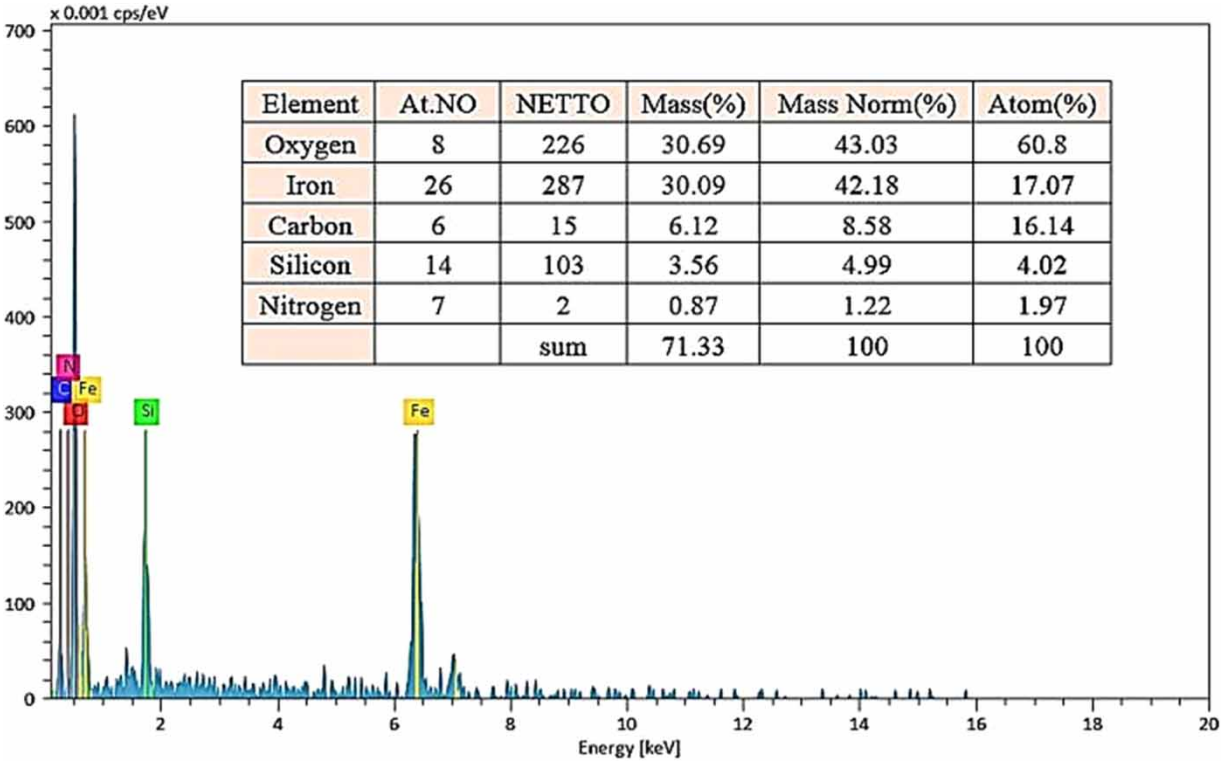

Element	At.NO	NETTO	Mass(%)	Mass Norm(%)	Atom(%)
Oxygen	8	226	30.69	43.03	60.8
Iron	26	287	30.09	42.18	17.07
Carbon	6	15	6.12	8.58	16.14
Silicon	14	103	3.56	4.99	4.02
Nitrogen	7	2	0.87	1.22	1.97
		sum	71.33	100	100

Figure 6 | EDS spectrum of MNPs of Fe_3O_4–SiO_2–NH_2.

and recovery activity decrease with increasing enzyme concentration. For the reason that after saturation of the nanoparticles capacity to bind the enzyme, the residual enzyme concentration in the supernatant of the immobilization solution increases and reduces immobilization yield and activity recovery. The lower-activity immobilized 1IMP-1 may be due to conformational changes in the enzyme's active site as a result of strong covalent bonds between the enzyme and the carrier (Zhang *et al.* 2013). Also, the free enzyme may experience protein aggregation (mainly near the isoelectric point). This may be because of undesired enzyme interactions where inactivation can stabilize incorrect enzyme structures (Siar *et al.* 2018). This manner was also reported in a 2016 study by Xiao *et al.*, in this study, activity of k-carrageenase immobilized onto magnetic iron oxide nanoparticles was lower than free enzyme (Xiao *et al.* 2016). The capacity of nanoparticles for the IMP-1 was 221 mg/g nanoparticles, which is more than the amount reported by Lee *et al.* (2011). The capacity of Ni magnetic nanoparticles for immobilization of six histidine-tagged enzyme was obtained at 36 mg enzyme/1 g nanoparticle . The improved binding capacity of the MNPs is probably caused by the high surface area of their nanostructure (Wang & Lin 2012).

Characterization of the free and immobilized IMP-1

Optimum pH and temperature

The data for determining the optimum pH of free IMP-1 showed that the optimum pH was 7.5 and changed to 6.5 after immobilization (Figure 7(a)). The relative activity of the immobilized enzyme at optimum pH (7.5) of the free enzyme was equal to 85% and for the free enzyme at optimum pH of immobilized enzyme was 90%. However, according to the optimum pH data, the immobilized enzyme had a suitable activity in the range of 6.5–7.5. The pH is one of the most important parameters that significantly affect the activity of enzymes. Normally, the enzyme activity changes due to the structural conversion of the immobilized enzyme in the optimum pH immobilization process. This change in the optimum pH value can be due to a change in the ionization of the basic and acidic amino acid side chains in the perimeter around the active site of the enzyme (Mazlan & Hanifah 2017). According to the results, the optimum temperatures of free and immobilized enzymes were 70 °C and 60 °C, respectively (Figure 7(b)). However, no significant difference was observed in the immobilized

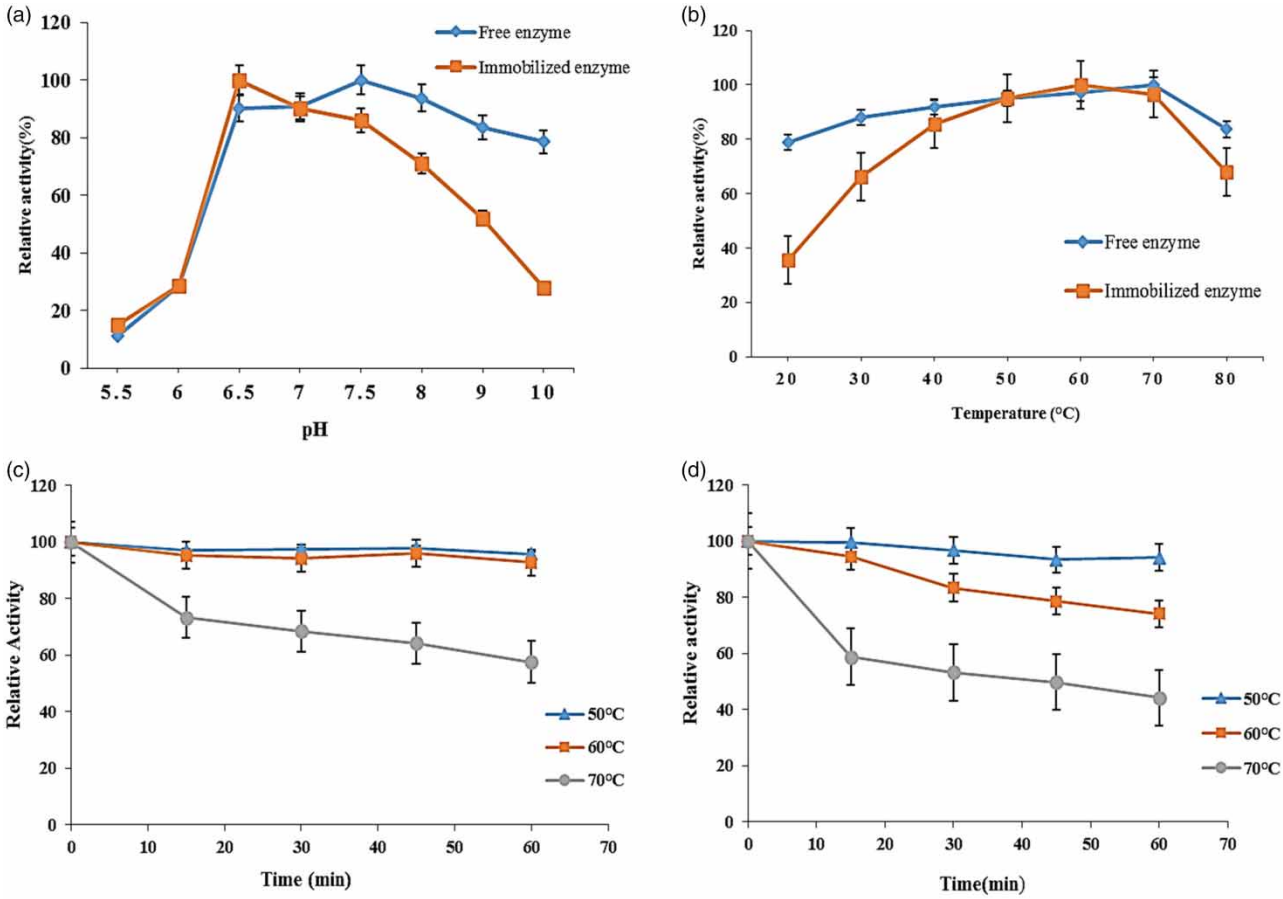

Figure 7 | Optimum pH and (a) optimum temperature of free and immobilized IMP-1 activity (b), thermal stability of free IMP-1 (c), thermal stability of immobilized IMP-1 (d).

enzyme activity at temperatures of 50, 60, and 70 °C. Differences in the optimum pH and temperature after immobilization has been reported by other study (Bussamara *et al.* 2012). Various factors may be responsible for these changes, such as the three-dimensional enzyme structural changes that possibly occur during the immobilization procedure. Although the optimum temperature for immobilized enzyme activity was lower than for free enzyme, the data suggest that the immobilized form of IMP-1 may be employed for environmental applications that do not need high temperatures.

Thermal stability of the free and immobilized IMP-1

The results showed the thermal stability of the IMP-1 decreased after immobilization. The immobilized enzyme retains 44.2% of its initial activity after 1 hour at 70 °C, while this amount is about 57.14% for the free enzyme (Figure 7(c) and 7(d)). In addition, at 50 °C and at different times, no significant difference was observed in the relative activity of free and immobilized enzymes. At 60 and 70 °C, the relative activity of free and immobilized enzymes decreased with increasing incubation time, but the slope of reduced activity for the immobilized enzyme was higher than the free enzyme. The results of this study showed that after immobilization of the enzyme, its thermal stability is reduced, but there is no significant difference in the thermal stability of the free and immobilized enzymes at 50 °C. At 60 °C the stability of the free enzyme was slightly higher than that of the immobilized enzyme, and this difference was evident at 70 °C. With regards to the application temperature of the biocatalyst for antibiotic removal is not high and is at ambient temperature, this decrease stability at 70 °C can be neglected. The decrease in thermal stability of the enzyme after immobilization may be due to the fact that after high-temperature incubation, the activity was measured at 25 °C and the immobilized enzyme could not recover due to binding to the carrier. In the study of Kanbar & Ozdemir (2010), a decrease in the thermal stability of the carbonic anhydrase enzyme was reported after immobilization (Kanbar & Ozdemir 2010).

Reusability and storage stability

The immobilization of enzymes has provided several advantages compared to free enzymes: stable biocatalysts, production efficiency, the possibility of reuse, and easy purification of the products. The reusability of enzyme particles is very important when considering enzymatic reactions. Enzyme reusability was considered for continuous enzyme use. Reusability studies showed that some of its activity was reduced after each cycle of immobilized enzyme use. After 15 reuse cycles, 80% of the initial activity was maintained. Various factors are effective in reducing the relative activity of immobilized enzymes after use cycles. In this study, a part of the nanobiocatalyst may have been reduced due to the use of an external magnet to separate the nanobiocatalyst from the reaction solution after each cycle and wash for reuse for the next cycle. This problem can reduce the relative activity of the immobilized enzyme after successive cycles of reuse and washing (Figure 8(b)). Storage stability data of free and immobilized enzyme showed that in the first week of storage time, there is a significant difference in reducing the activity of immobilized enzyme compared to the free enzyme, but in the following weeks, no significant reduction was observed.ed enzyme. After 4 weeks of storage at 4 °C, immobilized IMP-1 retained more than 74% of its initial activity, while the free enzyme value was 80%. However, in a similar study, a decrease in the relative activity of the immobilized TEM-1 enzyme on magnetic nanoparticles was reported to be 70% after 16 days of storage at 4 °C (Gao *et al.* 2018) which is higher than the amount obtained in the present study. This study observed that free IMP-1 also has appropriate storage stability without adding preservatives at 4 °C (Figure 8(a)). Factors such as organic solvents, temperature changes, and ionic strength can reduce the durability of biocatalysts. Also, enzymes are partially denatured in aqueous solutions, which leads to a decrease in their activity (Dias Gomes & Woodley 2019).

Kinetic parameter for Pen G, CEX, and CRO antibiotics

The velocity of reaction at the time the enzyme is saturated with the substrate, is considered the maximum velocity of the reaction (Vmax). The Michaelis constant (k_m) is the concentration of the substrate, when the reaction rate is half the maximum velocity. The K_m and V_{max} of free and immobilized IMP-1 were determined by Michaelis–Menten and Lineweaver-Burk plots (Figure 9). For free and immobilized enzymes, the highest catalytic activity was observed for Pen G and CEX, whereas Vmax/Km value for CRO was 3-fold (free enzyme) to 10-fold (immobilized enzyme) lower than for Pen G (Table 4). Also, the catalytic activity of the free enzyme (relative Vmax/Km) for CEX substrate is higher than Pen G and they are almost equal after immobility. When the enzyme is immobilized, issues of diffusion and transport arise. If there is an unstirred boundary layer near the surface, the substrate concentration at the surface may differ from the substrate concentration in the bulk fluid. In addition, the product will accumulate on the surface, potentially inhibiting the reaction. This can be a problem in a microfluidic situation, or with carriers of enzymes if they are not kept in motion. The higher the molecular weight of the substrate and product, the bigger the problem, since diffusion rates through the unstirred layer slow down as the molecules get larger. In addition, the free enzyme may experience protein aggregation (mainly near the isoelectric point). This may be caused by undesired enzyme interactions where inactivation can stabilize incorrect enzyme structures (Sanchez *et al.* 2016).

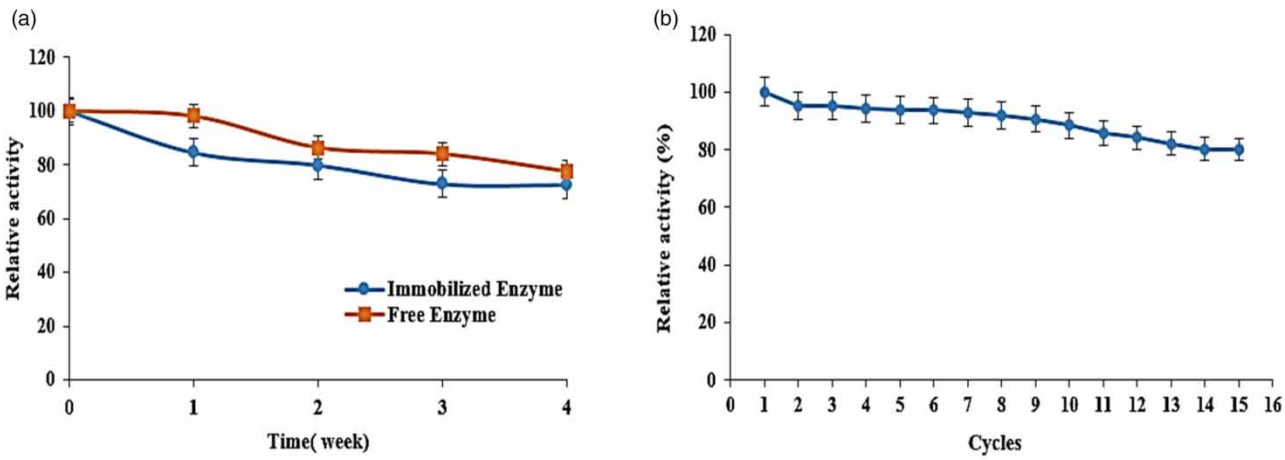

Figure 8 | Storage stability of the free and the immobilized IMP-1 (a), Recyclability of immobilized IMP-1 (b).

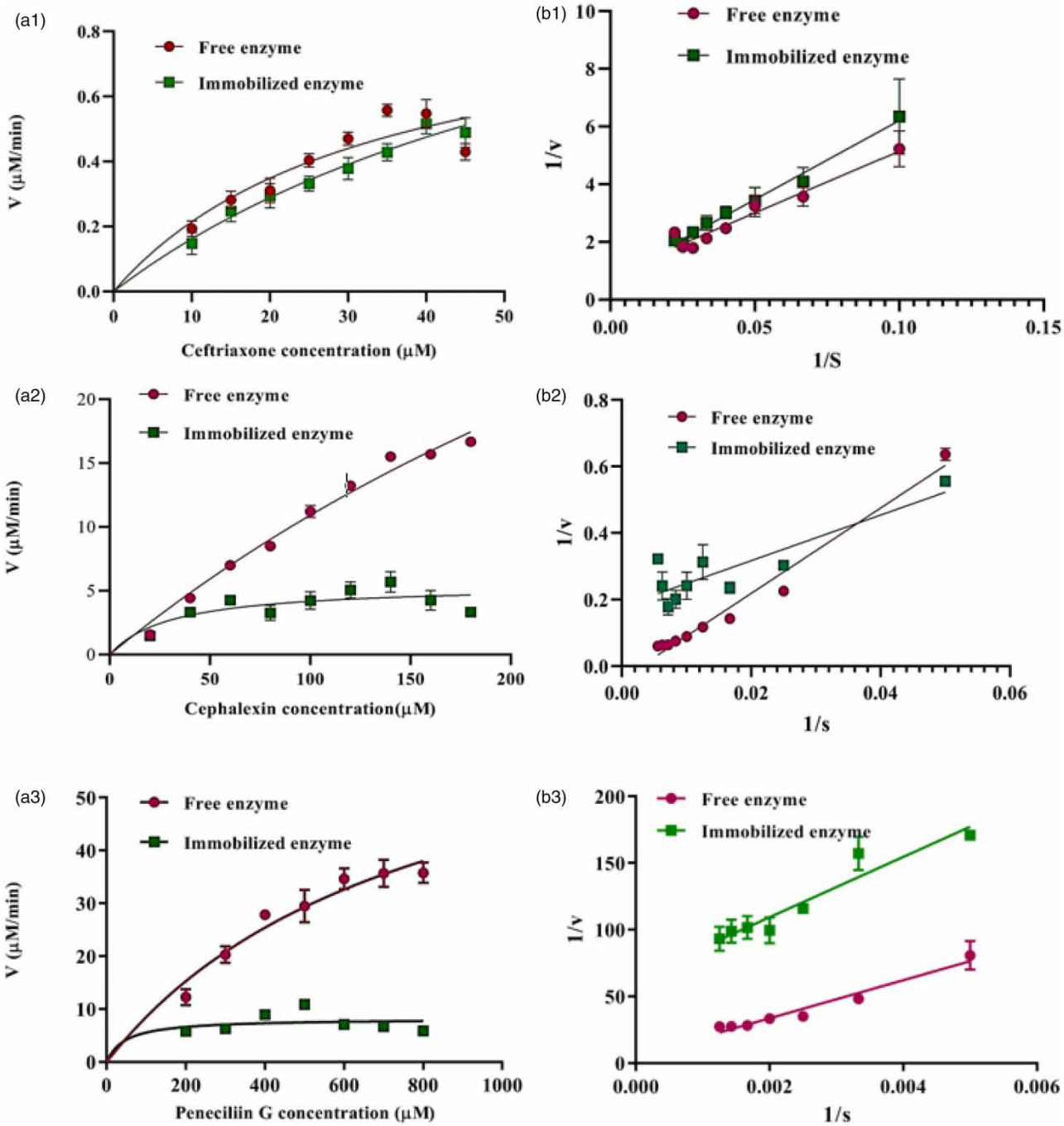

Figure 9 | Michaelis-Menten (a) and Lineweaver-Burk plots (b) of the free and immobilized IMP-1: CRO (A1, B1), CEX (A2, B2), Pen G (A3, B3).

This requirement may be easily met in the flow-through system with immobilized enzymes because the substrate is continually replenished (Cooney 2011). In the current study, the decrease in the value of V_{max} for Pen G and CEX after immobilization of IMP-1 may be due to the substrate diffusion limit (Nematian *et al.* 2020). This manner has been reported in other studies for enzymes that are immobilized in various carriers (Kharel *et al.* 2004). Moreover, after immobilization, IMP-1 on the carrier was significantly reduced the K_m value, indicating a greater enzyme-substrate affinity which may be because of conformational changes of the enzyme resulting in a higher affinity of these substrates for the IMP-1. However, this decrease was also observed in K_m in another study for lipase immobilization (Aghababaie *et al.* 2018).

Table 4 | Kinetic parameters for beta-lactam antibiotic with free and immobilized IMP-1

	Substrate	V_{max} ($\mu M.min^{-1}$)	Relative V_{max}	Km (μM)	Relative V_{max}/K_m ($\mu M^{-1}\ min^{-1}$)
free enzyme	Penicillin G	75.50	100	789	100
	Cephalexin	69.13	90.27	533.6	135
	Ceftriaxone	0.9294	1.23	33.34	29
immobilized enzyme	Penicillin G	8.215	100	47.7 ±	100
	Cephalexin	5.459	66.5	31	103
	Ceftriaxone	1.336	16.2	72.55	10.82

On the contrary of the Pen G and CEX, K_m and V_{max} of IMP-1 for CRO were increased after immobilization. The free and immobilized IMP-1 for CRO is significantly lower than that of Pen G and CEX, indicating that the IMP-1 is more affinity to CRO. However, K_m and V_{max} of the IMP-1 increased after immobilization (decreased affinity). This may be due to changes in the three-dimensional conformation of the active site at the immobilized enzyme which has increased access to this substrate (Guzik *et al.* 2014).

Enzymatic inactivation of beta-lactam antibiotics

The beta-lactamase activity differs from that found in *Enterobacteriaceae* and *Pseudomonas*. In the present study, the agar well diffusion method was used to evaluate the beta-lactamase effect of IMP-1 on the studied antibiotics. The comparison of the diameter of the zone of inhibition of growth of the *E. coli* between antibiotics and their enzymatic hydrolysis products showed that the antibiotics were inactivated due to the enzymatic hydrolysis. Enzyme function is carried out by the opening of the beta-lactam ring. This ring plays a key role in inhibiting cell wall synthesis and leads to bacterial death (Fuda *et al.* 2005).

CONCLUSION

The present study was performed to develop a novel nanobiocatalyst by immobilizing IMP-1 metallo-beta-lactamase on the magnetic nanoparticles to remove beta-lactam antibiotics from aqueous solutions. For this purpose, the recombinant IMP-1 was produced by overexpression of the bla_{IMP} gene cloned into the pET28a vector in *E. coli* and purified.

Purified IMP-1 was immobilized on the Synthesized and functionalized Fe_3O_4@SiO_2 nanoparticles by covalent cross-linking process and used to degrade three beta-lactam antibiotics. The HRTEM, FTIR, and EDS studies of the synthesized magnetic nanoparticles show that the synthesis, functionalization, activation of the nanoparticles as enzyme carriers were performed successfully. The optimum pH of free and immobilized enzyme activity was 7.5 and 6.5, respectively, and the optimum temperature of free and immobilized enzyme activity was 70 and 60 °C, respectively. Also, no significant difference was observed in the thermal stability of the enzyme after immobilization at 50 and 60 °C. The immobilized enzyme retained 44.2% of its original activity after one hour at 70 °C, compared with about 57.14% for the free enzyme. No significant difference was observed in the storage stability of immobilized and free enzymes. After 4 weeks of storage at 4 °C, the relative activity of the immobilized enzyme was 73%, while that for the free enzyme was 80%. The immobilized enzyme was reusable and after 15 cycles of reuse had an 80% relative activity. The kinetic parameters (K_m and V_{max}) for the three studied antibiotics showed that the enzymatic hydrolysis rate of Pen G, CEX, and CRO is reduced by the enzyme, respectively. The results also showed that these antibiotics were completely inactivated by enzymatic hydrolysis. The results of this study also showed that the enzymatic process using IMP-1 enzyme immobilized on silica-modified magnetic nanoparticles can be used as a promising approach with high efficiency and inexpensive to remove beta-lactam antibiotics from aqueous solutions. Thus, this nanocatalyst could be an appropriate choice for removing beta-lactam antibiotics from pharmaceutical industry wastewater.

AUTHOR CONTRIBUTION STATEMENT

R.K., A.A., and M.S. designed the study. M.S. and F.K. carried out the experiments. M.S. wrote the manuscript with support from R.K. and F.K., and S.M. All authors discussed the results and contributed to the final manuscript.

ACKNOWLEDGEMENTS

The authors gratefully acknowledge Kermanshah University of Medical Science (Grant Number: 990080) for the financial support. This work was performed in partial fulfillment of the requirement for the environmental health engineering Ph.D. of Mohammad javad Shokoohizadeh, in Faculty of Health, Kermanshah University of Medical Sciences, Kermanshah, Iran.

DATA AVAILABILITY STATEMENT

All relevant data are included in the paper or its Supplementary Information.

REFERENCES

Aghababaie, M., Beheshti, M., Bordbar, A.-K. & Razmjou, A. 2018 Novel approaches to immobilize Candida rugosa lipase on nanocomposite membranes prepared by covalent attachment of magnetic nanoparticles on poly acrylonitrile membrane. *RSC Advances* **8** (9), 4561–4570.

Alemi-Tameh, F., Safaei-Ghomi, J., Mahmoudi-Hashemi, M. & Teymuri, R. 2016 A comparative study on the catalytic activity of Fe_3O_4@ SiO_2–SO_3 H and Fe_3O_4@ SiO_2–NH_2 nanoparticles for the synthesis of spiro [chromeno [2, 3-c] pyrazole-4, 3′-indoline]-diones under mild conditions. *Research on Chemical Intermediates* **42** (7), 6391–6406.

Al-Gheethi, A. A., Lalung, J., Noman E, A., Bala, J. & Norli, I. 2015 Removal of heavy metals and antibiotics from treated sewage effluent by bacteria. *Clean Technologies and Environmental Policy* **17** (8), 2101–2123.

Arjomandi, O. K., Kavoosi, M. & Adibi, H. 2019 Synthesis and investigation of inhibitory activities of imidazole derivatives against the metallo-β-lactamase IMP-1. *Bioorganic Chemistry* **92**, 103277.

Barbosa, O., Ortiz, C., Berenguer-Murcia, Á., Torres, R., Rodrigues, R. C. & Fernandez-Lafuente, R. 2014 Glutaraldehyde in bio-catalysts design: a useful cross-linker and a versatile tool in enzyme immobilization. *RSC Advances* **4** (4), 1583–1600.

Becker, D., Della Giustina, S. V., Rodriguez-Mozaz, S., Schoevaart, R., Barceló, D., de Cazes, M., Belleville, M. P., Sanchez-Marcano, J., de Gunzburg, J., Couillerot, O., Völker, J. & Wagner, M. 2016 Removal of antibiotics in wastewater by enzymatic treatment with fungal laccase–degradation of compounds does not always eliminate toxicity. *Bioresource Technology* **219**, 500–509.

Bilal, M., Ashraf, S. S., Barceló, D. & Iqbal, H. M. 2019 Biocatalytic degradation/redefining 'removal' fate of pharmaceutically active compounds and antibiotics in the aquatic environment. *Science of the Total Environment* **691**, 1190–1211.

Bradford, M. 1976 A rapid and sensitive method for the quantitation of microgram quantities of protein utilizing Cancer Res 2006; 66:(7). April 1, 2006 3462 www. aacrjournals. org the principle of protein-dye binding. *Anal Biochem* **72**, 248–254.

Bussamara, R., Dall'Agnol, L., Schrank, A., Fernandes, K. F. & Vainstein, M. H. 2012 Optimal conditions for continuous immobilization of Pseudozyma hubeiensis (strain HB85A) lipase by adsorption in a packed-bed reactor by response surface methodology. *Enzyme Research* **2012**, 1–12.

Chen, F.-H., Gao, Q. & Ni, J. 2008 The grafting and release behavior of doxorubincin from Fe_3O_4@ SiO_2 core–shell structure nanoparticles via an acid cleaving amide bond: the potential for magnetic targeting drug delivery. *Nanotechnology* **19** (16), 165103.

Chen, C., Sun, W., Lv, H., Li, H., Wang, Y. & Wang, P. 2018 Spacer arm-facilitated tethering of laccase on magnetic polydopamine nanoparticles for efficient biocatalytic water treatment. *Chemical Engineering Journal* **350**, 949–959.

Cooney, M. J. 2011 Kinetic measurements for enzyme immobilization. *Enzyme Stabilization and immobilization* **679**, 207–225.

Couto, C. F., Lange, L. C. & Amaral, M. C. S. 2018 A critical review on membrane separation processes applied to remove pharmaceutically active compounds from water and wastewater. *Journal of Water Process Engineering* **26**, 156–175.

Crini, G., Lichtfouse, E., Wilson, L. D. & Morin-Crini, N. 2019 Conventional and non-conventional adsorbents for wastewater treatment. *Environmental Chemistry Letters* **17** (1), 195–213.

Cui, J., Ren, S., Sun, B. & Jia, S. 2018 Optimization protocols and improved strategies for metal-organic frameworks for immobilizing enzymes: current development and future challenges. *Coordination Chemistry Reviews* **370**, 22–41.

De Rosa, M., Verdino, A., Soriente, A. & Marabotti, A. 2021 The odd couple (s): an overview of beta-lactam antibiotics bearing more than one pharmacophoric group. *International Journal of Molecular Sciences* **22** (2), 617.

Dias Gomes, M. & Woodley, J. M. 2019 Considerations when measuring biocatalyst performance. *Molecules* **24** (19), 3573.

Elander, R. 2003 Industrial production of β-lactam antibiotics. *Applied Microbiology and Biotechnology* **61** (5), 385–392.

Fang, G., Chen, H., Zhang, Y. & Chen, A. 2016 Immobilization of pectinase onto Fe_3O_4@ SiO_2–NH_2 and its activity and stability. *International Journal of Biological Macromolecules* **88**, 189–195.

Feyzi, M. & Norouzi, L. 2016 Preparation and kinetic study of magnetic Ca/Fe_3O4@ SiO_2 nanocatalysts for biodiesel production. *Renewable Energy* **94**, 579–586.

Froger, A. & Hall, J. E. 2007 Transformation of plasmid DNA into E. coli using the heat shock method. *Journal of Visualized Experiments: JoVE* (6).

Fuda, C., Fisher, J. & Mobashery, S. 2005 β-Lactam resistance in Staphylococcus aureus: the adaptive resistance of a plastic genome. *Cellular and Molecular Life Sciences* **62** (22), 2617–2633.

Gallagher, S. R. & Wiley, E. A. 2010 *Current Protocols Essential Laboratory Techniques*. John Wiley & Sons, Hoboken, NJ, USA.

Gao, X., Fan, X., Chen, X. & Ge, Z. 2018 Immobilized β-lactamase on Fe_3O_4 magnetic nanoparticles for degradation of β-lactam antibiotics in wastewater. *International Journal of Environmental Science and Technology* **15** (10), 2203–2212.

Gemeay, A. H., Keshta, B. E., El-Sharkawy, R. G. & Zaki, A. B. 2020 Chemical insight into the adsorption of reactive wool dyes onto amine-functionalized magnetite/silica core-shell from industrial wastewaters. *Environmental Science and Pollution Research* **27** (26), 32341–32358.

Ghasemzadeh, M. A., Abdollahi-Basir, M. H. & Babaei, M. 2015 Fe_3O_4@ SiO_2–NH_2 core-shell nanocomposite as an efficient and green catalyst for the multi-component synthesis of highly substituted chromeno [2, 3-b] pyridines in aqueous ethanol media. *Green Chemistry Letters and Reviews* **8** (3–4), 40–49.

Gnanamani, A., Hariharan, P. & Paul-Satyaseela, M. 2017 Staphylococcus aureus: overview of bacteriology, clinical diseases, epidemiology, antibiotic resistance and therapeutic approach. *Frontiers in Staphylococcus Aureus* **4**, 28.

Guzik, U., Hupert-Kocurek, K. & Wojcieszyńska, D. 2014 Immobilization as a strategy for improving enzyme properties-application to oxidoreductases. *Molecules* **19** (7), 8995–9018.

Homem, V. & Santos, L. 2011 Degradation and removal methods of antibiotics from aqueous matrices–a review. *Journal of Environmental Management* **92** (10), 2304–2347.

Horton, L. B., Shanker, S., Mikulski, R., Brown, N. G., Phillips, K. J., Lykissa, E., Venkataram, P. B. & Palzkill, T. 2012 Mutagenesis of zinc ligand residue Cys221 reveals plasticity in the IMP-1 metallo-β-lactamase active site. *Antimicrobial Agents and Chemotherapy* **56** (11), 5667–5677.

Kanbar, B. & Ozdemir, E. 2010 Thermal stability of carbonic anhydrase immobilized within polyurethane foam. *Biotechnology Progress* **26** (5), 1474–1480.

Kharel, M.-K., Liou, K.-K., Sohng, J.-K. & Lee, H.-C. 2004 Production of dTDP-4-keto-6-deoxy-D-glucose by immobilization of dTDP-D-glucose 4, 6-dehydratase. *Journal of Microbiology and Biotechnology* **14** (2), 297–301.

Lateef, A. 2004 The microbiology of a pharmaceutical effluent and its public health implications. *World Journal of Microbiology and Biotechnology* **20** (2), 167–171.

Lee, S. Y., Lee, S., Kho, I. H., Lee, J. H., Kim, J. H. & Chang, J. H. 2011 Enzyme–magnetic nanoparticle conjugates as a rigid biocatalyst for the elimination of toxic aromatic hydrocarbons. *Chemical Communications* **47** (36), 9989–9991.

Lima, G. V., da Silva, M. R., Fonseca, T. d. S., de Lima, L. B., de Oliveira, M. d. C. F., de Lemos, T. L. G., Zampieri, D., dos Santos, J. C. S., Rios, N. S. & Gonçalves, L. R. B. 2017 Chemoenzymatic synthesis of (S)-Pindolol using lipases. *Applied Catalysis A: General* **546**, 7–14.

Lomovskaya, O., Tsivkovski, R., Nelson, K., Rubio-Aparicio, D., Sun, D., Totrov, M. & Dudley, M. N. 2020 Spectrum of beta-lactamase inhibition by the cyclic boronate QPX7728, an ultrabroad-spectrum beta-lactamase inhibitor of serine and metallo-beta-lactamases: enhancement of activity of multiple antibiotics against isogenic strains expressing single beta-lactamases. *Antimicrobial Agents and Chemotherapy* **64** (6), e00212–e00220.

Lu, Y., He, B., Shen, J., Li, J., Yang, W. & Yin, M. 2015 Multifunctional magnetic and fluorescent core–shell nanoparticles for bioimaging. *Nanoscale* **7** (5), 1606–1609.

Ma, M., Zhang, Y., Yu, W., Shen, H.-y., Zhang, H.-q. & Gu, N. 2003 Preparation and characterization of magnetite nanoparticles coated by amino silane. *Colloids and Surfaces A: Physicochemical and Engineering Aspects* **212** (2–3), 219–226.

Mazlan, S. Z. & Hanifah, S. A. 2017 Effects of temperature and pH on immobilized laccase activity in conjugated methacrylate-acrylate microspheres. *International Journal of Polymer Science* **2017**.

Melo, A. D., Silva, F. F., Dos Santos, J., Fernández-Lafuente, R., Lemos, T. L. & Dias Filho, F. A. 2017 Synthesis of benzyl acetate catalyzed by lipase immobilized in nontoxic chitosan-polyphosphate beads. *Molecules* **22** (12), 2165.

Messasma, Z., Ourari, A., Mahdadi, R., Houchi, S., Aggoun, D., Kherbache, A. & Bentouhami, E. 2018 Synthesis, spectral characterization, DFT computational studies and inhibitory activity of novel N2S2 tetradentates Schiff bases on metallo-beta-lactamases of Acinetobacter baumannii. *Journal of Molecular Structure* **1171**, 672–681.

Mojica, M. F., Rossi, M.-A., Vila, A. J. & Bonomo, R. A. 2006 Doctopic: review and opinion. *Concern* **30**, 31.

Monteiro, R. R., Neto, D. M. A., Fechine, P., Lopes, A. A., Gonçalves, L. R., dos Santos, J., de Souza, M. & Fernandez-Lafuente, R. 2019 Ethyl butyrate synthesis catalyzed by lipases A and B from Candida antarctica immobilized onto magnetic nanoparticles. improvement of biocatalysts' performance under ultrasonic irradiation. *International Journal of Molecular Sciences* **20** (22), 5807.

Nandiyanto, A. B. D., Oktiani, R. & Ragadhita, R. 2019 How to read and interpret FTIR spectroscope of organic material. *Indonesian Journal of Science and Technology* **4** (1), 97–118.

Nematian, T., Shakeri, A., Salehi, Z. & Saboury, A. A. 2020 Lipase immobilized on functionalized superparamagnetic few-layer graphene oxide as an efficient nanobiocatalyst for biodiesel production from Chlorella vulgaris bio-oil. *Biotechnology for Biofuels* **13** (1), 1–15.

Pandey, K., Singh, B., Pandey, A. K., Badruddin, I. J., Pandey, S., Mishra, V. K. & Jain, P. A. 2017 Application of microbial enzymes in industrial waste water treatment. *International Journal of Current Microbiology and Applied Sciences* **6** (8), 1243–1254.

Pirsaheb, M., Khamutian, R. & Khodadadian, M. 2014 A comparison between extended aeration sludge and conventional activated sludge treatment for removal of linear alkylbenzene sulfonates (Case study: Kermanshah and Paveh WWTP). *Desalination and Water Treatment* **52** (25–27), 4673–4680.

Riaz, L., Anjum, M., Yang, Q., Safeer, R., Sikandar, A., Ullah, H., Shahab, A., Yuan, W. & Wang, Q. 2020 Treatment technologies and management options of antibiotics and AMR/ARGs. In: *Antibiotics and Antimicrobial Resistance Genes in the Environment* (Hashmi, M. Z., ed.). Elsevier, Amsterdam, Netherlands. pp. 369–393.

Ribeiro, A. R., Sures, B. & Schmidt, T. C. 2018 Cephalosporin antibiotics in the aquatic environment: a critical review of occurrence, fate, ecotoxicity and removal technologies. *Environmental Pollution* **241**, 1153–1166.

Rodriguez, J. M. G., Hux, N. P., Philips, S. J. & Towns, M. H. 2019 Michaelis–Menten graphs, lineweaver–Burk plots, and reaction schemes: investigating introductory biochemistry students' conceptions of representations in enzyme kinetics. *Journal of Chemical Education* **96** (9), 1833–1845.

Rodriguez-Mozaz, S., Chamorro, S., Marti, E., Huerta, B., Gros, M., Sànchez-Melsió, A., Borrego, C. M., Barceló, D. & Balcázar, J. L. 2015 Occurrence of antibiotics and antibiotic resistance genes in hospital and urban wastewaters and their impact on the receiving river. *Water Research* **69**, 234–242.

Rueda, N., Albuquerque, T. L., Bartolome-Cabrero, R., Fernandez-Lopez, L., Torres, R., Ortiz, C., Dos Santos, J., Barbosa, O. & Fernandez-Lafuente, R. 2016 Reversible immobilization of lipases on heterofunctional octyl-amino agarose beads prevents enzyme desorption. *Molecules* **21** (5), 646.

Sanchez, A., Cruz, J., Rueda, N., dos Santos, J. C., Torres, R., Ortiz, C., Villalonga, R. & Fernandez-Lafuente, R. 2016 Inactivation of immobilized trypsin under dissimilar conditions produces trypsin molecules with different structures. *RSC Advances* **6** (33), 27329–27334.

Schlesinger, S. R., Kim, S. G., Lee, J.-S. & Kim, S.-K. 2011 Purification development and characterization of the zinc-dependent metallo-β-lactamase from Bacillus anthracis. *Biotechnology Letters* **33** (7), 1417–1422.

Sheldon, R. & van Pelt, S. 2013 Evaluation of immobilized enzymes for industrial applications. *Chemical Society Reviews* **15**, 6223–6235.

Shokoohi, R., Samadi, M. T., Amani, M. & Poureshgh, Y. 2018 Modeling and optimization of removal of cefalexin from aquatic solutions by enzymatic oxidation using experimental design. *Brazilian Journal of Chemical Engineering* **35**, 943–956.

Siar, E.-H., Arana-Peña, S., Barbosa, O., Zidoune, M. N. & Fernandez-Lafuente, R. 2018 Immobilization/stabilization of ficin extract on glutaraldehyde-activated agarose beads. Variables that control the final stability and activity in protein hydrolyses. *Catalysts* **8** (4), 149.

Thai, P. K., Binh, V. N., Nhung, P. H., Nhan, P. T., Hieu, N. Q., Dang, N. T., Tam, N. K. B. & Anh, N. T. K. 2018 Occurrence of antibiotic residues and antibiotic-resistant bacteria in effluents of pharmaceutical manufacturers and other sources around Hanoi, Vietnam. *Science of the Total Environment* **645**, 393–400.

Wahab, R. A., Elias, N., Abdullah, F. & Ghoshal, S. K. 2020 On the taught new tricks of enzymes immobilization: an all-inclusive overview. *Reactive and Functional Polymers* **152**, 104613.

Waley, S. G. 1974 A spectrophotometric assay of β-lactamase action on penicillins. *Biochemical Journal* **139** (3), 789–790.

Wang, X.-H. & Lin, A. Y.-C. 2012 Phototransformation of cephalosporin antibiotics in an aqueous environment results in higher toxicity. *Environmental Science & Technology* **46** (22), 12417–12426.

Xiao, A., Xu, C., Lin, Y., Ni, H., Zhu, Y. & Cai, H. 2016 Preparation and characterization of κ-carrageenase immobilized onto magnetic iron oxide nanoparticles. *Electronic Journal of Biotechnology* **19** (1), 1–7.

Yang, B., Zuo, J., Li, P., Wang, K., Yu, X. & Zhang, M. 2016 Effective ultrasound electrochemical degradation of biological toxicity and refractory cephalosporin pharmaceutical wastewater. *Chemical Engineering Journal* **287**, 30–37.

Zhanel, G. G., Lawson, C. D., Adam, H., Schweizer, F., Zelenitsky, S., Lagacé-Wiens, P. R., Denisuik, A., Rubinstein, E., Gin, A. S. & Hoban, D. J. 2013 Ceftazidime-avibactam: a novel cephalosporin/β-lactamase inhibitor combination. *Drugs* **73** (2), 159–177.

Zhang, D.-H., Yuwen, L.-X. & Peng, L.-J. 2013 Parameters affecting the performance of immobilized enzyme. *Journal of Chemistry* **2013**.

Zhang, Q., Yang, X. & Guan, J. 2019 Applications of magnetic nanomaterials in heterogeneous catalysis. *ACS Applied Nano Materials* **2** (8), 4681–4697.

Zhang, C., Zhao, Z., Dong, S. & Zhou, D. 2021 Simultaneous elimination of amoxicillin and antibiotic resistance genes in activated sludge process: contributions of easy-to-biodegrade food. *Science of the Total Environment* **764**, 142907.

Zhao, Z., Feng, Y., Shamsaei, E., Song, J., Wang, H. & He, L. 2016 Highly stable enzymatic membrane for fast treatment of antibiotic-polluted water. *Journal of Membrane Science* **518**, 1–9.

Zhou, W., Rao, Y., Zhuang, W., Ge, L., Lin, R., Tang, T., Wu, J., Li, M., Yang, P. & Zhu, C. 2021 Improved enzymatic activity by oriented immobilization on graphene oxide with tunable surface heterogeneity. *Composites Part B: Engineering* **216**, 108788.

First received 5 December 2021; accepted in revised form 10 March 2022. Available online 22 March 2022